Journal of Sound and Vibration (1999) **222**(2), 171–189
Article No. jsvi.1998.2080, available online at http://www.idealibrary.com on IDEAL

VIBRATION CONTROL OF A FOUR-BAR MECHANISM WITH A FLEXIBLE COUPLER LINK

M. KARKOUB AND A. S. YIGIT
Department of Mechanical and Industrial Engineering, Kuwait University, P.O. Box 5969, *Safat*, 13060, *Kuwait*

(*Received* 16 *July* 1998, *and in final form* 22 *September* 1998)

Dynamic modelling and controller design for a flexible four-bar mechanism is studied. The fully coupled non-linear equations of motion are obtained through a constrained Lagrangian approach. Resulting differential-algebraic equations are solved numerically to obtain the system response. A linearized dynamic model is developed which facilitates the design of various controllers. The fully coupled nature of the governing equations facilitates control of elastic motion through the input link alone. A simple PD controller is designed based on a linearized model. These gains are subsequently tuned using the actual model to achieve the desired response. The resultant controller is shown to be efficient in suppressing the vibrations of the flexible link as well as controlling the rigid body motion.

1. INTRODUCTION

Four-bar mechanisms are widely used in the industry and can be found in machines such as photocopiers and card feeders [1]. The quest for high speed light weight machinery requires a redesign of the current mechanisms. Unfortunately, reducing the weight of four-bar mechanisms and/or increasing their speed may lead to the onset of elastic oscillations which causes performance degradation such as misfeeding in the case of the card feeder mechanism [1]. Moreover, the dynamics of these mechanisms become more involved and make the control process a challenging task. Suppressing the vibrations of the coupler mid-point of a four-bar mechanism using torque actuators mounted on the input link is the subject of this work.

Traditionally, dynamic analysis and control of mechanisms have been based on the assumption that the links behave as rigid bodies. In mechanical systems operating at high speeds, some oscillatory elastic motion is inevitable. This motion becomes a major concern when performance requirements are such that high precision is important. Because of the trend toward increasing operating speeds and reducing weights in modern machinery, it may be inaccurate to treat certain links in such systems as rigid bodies. The effect of flexibility on the

0022–460X/99/170171 + 19 $30.00/0

dynamic behavior of mechanical systems has been the subject of numerous investigations (see e.g., reference [2]). Mathematical modelling of flexible mechanisms is complicated. The rigid body motion involves changing geometries resulting in varying system parameters, and these influence the elastic deformations. The elastic deformations themselves in turn influence the rigid body motion [3]. Though the importance of including the effect of elastic motion in dynamic modelling has been recognized for quite some time, most models were based on a prescribed rigid body motion (see e.g., references [4] and [5]). The assumption here is that the elastic deformations do not have significant effect on rigid body motion. In other words, there is only a one-way coupling between elastic deformations and rigid body motion. For lightweight and high-speed mechanisms where there are no large flywheel type inertia elements to maintain the rigid body motion independent of the elastic deformations, this modelling approach results in gross errors [6, 7]. Furthermore, in a control system formulation, this type of modelling results in an unobservable system with respect to the rigid body motion. Therefore, in these cases, a fully coupled formulation is essential. There are two distinct modelling approaches to fully coupled formulations. The first one is a finite element formulation where both rigid and elastic degrees of freedoms are considered as generalized co-ordinates [3]. The second approach uses the Lagrange multiplier technique to incorporate joint constraints into the equations of motion, and results in a mixed set of differential and algebraic equations (see e.g. reference [8]).

Although dynamic analysis of flexible mechanisms has been the subject of numerous investigations, the control of such systems has not received much attention. Sung and Chen [9] proposed an optimal control scheme to suppress the vibrations of a four-bar linkage with a flexible output link. They used piezoceramic sensors and actuators which are located on the flexible link. The effect of elastic deformations as well as control action on the rigid body motion was not considered since the authors used a model with only one-way coupling. Beale and Lee [10] investigated the feasibility of applying fuzzy control for a flexible slider–crank mechanism. A piezoelectric actuator placed on the flexible link was required to implement this controller. Liao *et al.* [11] also proposed the use of piezoelectric films and designed a robust controller based on a linearized state–space model of the mechanism. The effect of parameter variations and the instability caused by the control action is studied.

Most of the work available in the literature which deals with vibration control of flexible mechanisms employ an actuator which acts directly on the flexible link. The effect of the control forces and moments on the overall motion is neglected. In addition, the implementation of such controllers may require sophisticated and expensive design. An alternative method would be to control the vibrations through the motion of the input link. Since the elastic deformations are both observable and controllable through the rigid body motions with a fully coupled model, such a control strategy should be feasible. The current study deals with control of a four-bar mechanism with a very flexible coupler link. An actuator is assumed to be placed on the input link which applies a control torque. A simple PD control is designed which requires

measurement of the position and angular velocity of the input link only. This is different from the control technique proposed by Sung and Chen [9] where the actuator and the sensor are placed directly on the flexible link. Moreover, the control scheme proposed here controls both the flexible as well as the rigid body motion unlike the work done in reference [9] where the control of the rigid body motion is assumed to be done independently. It is evident from this study that the rigid body motion and the elastic deformations are strongly coupled; therefore, they need to be taken care of simultaneously. In this study, a constrained modelling approach is used. The elastic motion is treated by an assumed modes method instead of a finite element formulation. The resulting differential-algebraic equations are numerically solved for both open and closed-loop simulations. Simulation results demonstrate that the proposed controllers are effective in suppressing the vibrations as well as in accurate positioning of the mechanism.

2. DYNAMIC MODEL

The kinetic energy of the four-bar mechanism shown in Figure 1 is given by:

$$T = \frac{1}{2} I_c \dot{\theta}_2^2 + \frac{1}{2} I_o \dot{\theta}_4^4 + \frac{1}{2} \int_0^{l_3} \rho \dot{\mathbf{r}}^2 \, \mathrm{d}x, \tag{1}$$

where θ_2 and θ_4 are the input and output angles, respectively, I_c and I_o are the mass moments of inertia of the input and output links with respect to the joint

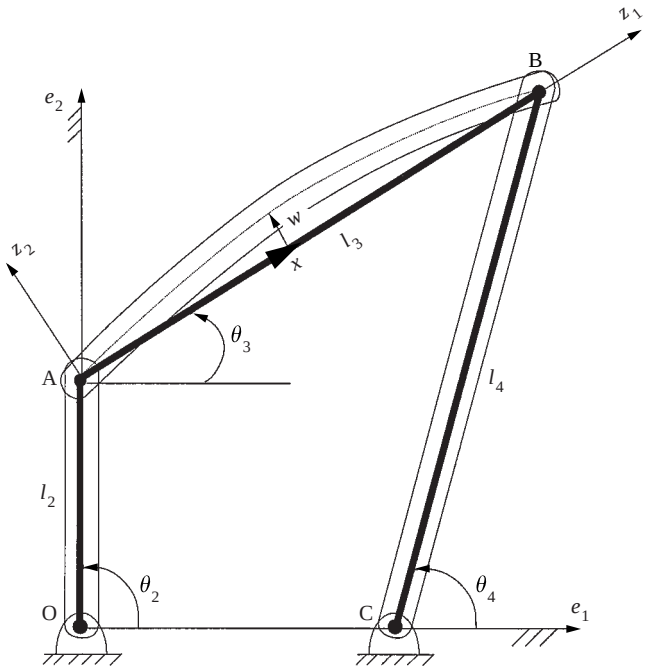

Figure 1. Sketch of the four-bar mechanism.

axes, respectively, ρ is mass per unit length of the coupler link, and $\mathbf{r}$ is the position vector of a point on the coupler link given as

$$\mathbf{r} = \mathbf{r}_2 + \mathbf{r}_3 + \mathbf{w}, \tag{2}$$

where

$$\mathbf{r}_2 = l_2 \cos(\theta_2)\mathbf{e}_1 + l_2 \sin(\theta_2)\mathbf{e}_2, \tag{3}$$

$$\mathbf{r}_3 = x \cos(\theta_3)\mathbf{e}_1 + x \sin(\theta_3)\mathbf{e}_2, \tag{4}$$

$$\mathbf{w} = w\mathbf{z}_2 \tag{5}$$

where w represents the elastic deformation of the coupler link at an arbitrary position x. The unit vectors $\mathbf{z}_1$ and $\mathbf{z}_2$ can be written as

$$\mathbf{z}_1 = \cos(\theta_3)\mathbf{e}_1 + \sin(\theta_3)\mathbf{e}_2, \tag{6}$$

$$\mathbf{z}_2 = -\sin(\theta_3)\mathbf{e}_1 + \cos(\theta_3)\mathbf{e}_2. \tag{7}$$

The strain energy is given by

$$U = \frac{1}{2}\int_0^{l_3} EI\left(\frac{\partial^2 w}{\partial x^2}\right)^2 \mathrm{d}x, \tag{8}$$

where EI is the flexural rigidity of the coupler link.

The variables θ_2, θ_3, and θ_4 are related by the following geometrical constraints:

$$\mathbf{\Phi} = \left\{ \begin{array}{l} -l_1 + l_2 \cos(\theta_2) + l_3 \cos(\theta_3) - l_4 \cos(\theta_4) \\ l_2 \sin(\theta_2) + l_3 \sin(\theta_3) - l_4 \sin(\theta_4) \end{array} \right\} = 0. \tag{9}$$

It should be noted that in general the constraint equations depend on the elastic deformations. However, because the longitudinal deformations are neglected and the transverse deformations are assumed small, the distance AB (see Figure 1) is assumed to be constant. Therefore, the constraint equations here do not depend on the elastic deformations.

The assumed modes method along with a constrained Lagrangian approach is used to obtain the discretized equations of motion. Let the deflection of the coupler link be written as

$$w(x, t) = \sum_{i=0}^{N} \psi_i(x) q_i(t), \tag{10}$$

where $q_i(t)$ are the modal co-ordinates and $\psi_i(x)$ are the mode shapes of a pinned–pinned beam given as

$$\psi_i(x) = \sin\left(\frac{i\pi}{l_3} x\right). \tag{11}$$

The constrained Lagrange's equations are

$$\frac{\mathrm{d}}{\mathrm{d}t}\left(\frac{\partial L}{\partial \dot{\eta}_i}\right) - \frac{\partial L}{\partial \eta_i} + \left(\frac{\partial \mathbf{\Phi}}{\partial \eta_i}\right)^T \mathbf{\Lambda} = F_i, \tag{12}$$

where

$$L = T - U,$$

and η_i are the generalized co-ordinates which includes rigid body co-ordinates as well as elastic modal co-ordinates. $\mathbf{\Phi}$ is the vector containing the constraint equations and $\mathbf{\Lambda}$ is the vector of Lagrange multipliers, λ_1 and λ_2; and F_i are the generalized forces. The force vector $(\partial \mathbf{\Phi}/\partial \eta_i)^T \mathbf{\Lambda}$ is substituted in to replace the removed joint forces.

The resulting differential equations are given as:

$$\begin{aligned}
&I_c\ddot{\theta}_2 + \rho l_2^2 l_3 \ddot{\theta}_2 + \frac{1}{2}\rho l_2 l_3^2 \ddot{\theta}_3 \cos(\theta_2 - \theta_3) - \frac{1}{2}\rho l_2 l_3^2 (\dot{\theta}_2 - \dot{\theta}_3)\dot{\theta}_3 \sin(\theta_2 - \theta_3) \\
&- l_2 \sin(\theta_2 - \theta_3)(\dot{\theta}_2 - \dot{\theta}_3) \sum_{i=1}^{N} \dot{q}_i Q_i + l_2 \cos(\theta_2 - \theta_3) \sum_{i=1}^{N} \ddot{q}_i Q_i \\
&+ l_2 \ddot{\theta}_3 \sin(\theta_2 - \theta_3) \sum_{i=1}^{N} q_i Q_i + l_2 \dot{\theta}_3 \cos(\theta_2 - \theta_3)(\dot{\theta}_2 - \dot{\theta}_3) \sum_{i=1}^{N} q_i Q_i \\
&+ l_2 \dot{\theta}_3 \sin(\theta_2 - \theta_3) \sum_{i=1}^{N} \dot{q}_i Q_i + l_2 \dot{\theta}_2 \sin(\theta_2 - \theta_3) \sum_{i=1}^{N} \dot{q}_i Q_i \\
&+ \frac{1}{2}\rho l_2 l_3^2 \dot{\theta}_2 \dot{\theta}_3 \sin(\theta_2 - \theta_3) - l_2 \dot{\theta}_2 \dot{\theta}_3 \sum_{i=1}^{N} \dot{q}_i Q_i - l_2 \sin(\theta_2)\lambda_1 + l_2 \cos(\theta_2)\lambda_2 = \tau,
\end{aligned} \tag{13}$$

$$\begin{aligned}
&\frac{1}{3}\rho l_3^3 \ddot{\theta}_3 + \sum_{i=1}^{N} \ddot{q}_i S_i + \ddot{\theta}_3 \sum_{i=1}^{N}\sum_{j=1}^{N} m_{ij} q_i q_j + \dot{\theta}_3 \sum_{i=1}^{N}\sum_{j=1}^{N} m_{ij} q_i q_j \\
&- \frac{1}{2}\rho l_2 l_3^2 \dot{\theta}_2 (\dot{\theta}_2 - \dot{\theta}_3) \sin(\theta_2 - \theta_3) + l_2 \ddot{\theta}_2 \sin(\theta_2 - \theta_3) \sum_{i=1}^{N} q_i Q_i \\
&+ l_2 \dot{\theta}_2 (\dot{\theta}_2 - \dot{\theta}_3) \cos(\theta_2 - \theta_3) \sum_{i=1}^{N} q_i Q_i + l_2 \dot{\theta}_2 \sin(\theta_2 - \theta_3) \sum_{i=1}^{N} \dot{q}_i Q_i \\
&- l_2 \dot{\theta}_2 \sin(\theta_2 - \theta_3) \sum_{i=1}^{N} \dot{q}_i Q_i - \frac{1}{2}\rho l_2 l_3^2 \dot{\theta}_2 \dot{\theta}_3 \sin(\theta_2 - \theta_3) + \frac{1}{2}\rho l_2 l_3^2 \ddot{\theta}_2 \cos(\theta_2 - \theta_3) \\
&- l_2 \dot{\theta}_2 \dot{\theta}_3 \cos(\theta_2 - \theta_3) \sum_{i=1}^{N} Q_i - l_3 \sin(\theta_3)\lambda_1 + l_3 \cos(\theta_3)\lambda_2 = 0,
\end{aligned} \tag{14}$$

$$I_o\ddot{\theta}_4 + l_4\sin(\theta_4)\lambda_1 - l_4\cos(\theta_4)\lambda_2 = 0, \tag{15}$$

$$\ddot{\theta}_3 S_i + \sum_{j=1}^{N} m_{ij}\ddot{q}_j + l_2\ddot{\theta}_2\cos(\theta_2 - \theta_3)Q_i$$

$$- l_3\dot{\theta}_2(\dot{\theta}_2 - \dot{\theta}_3)\sin(\theta_2 - \theta_3)Q_i - \dot{\theta}_3^2\sum_{j=1}^{N} m_{ij}q_j$$

$$- l_2\dot{\theta}_2\dot{\theta}_3\sin(\theta_2 - \theta_3)Q_i + \sum_{j=1}^{N} k_{ij}q_j = 0 \quad i = 1, 2, \ldots N, \tag{16}$$

where

$$Q_i = \int_0^{l_3} \rho\psi_i \, \mathrm{d}x, \qquad S_i = \int_0^{l_3} \rho x\psi_i \mathrm{d}x,$$

$$m_{ij} = \int_0^{l_3} \rho\psi_i\psi_j \, \mathrm{d}x, \quad k_{ij} = \int_0^{l_3} EI\psi_i^{''}\psi_j^{''} \, \mathrm{d}x,$$

and τ is the torque applied at the input joint.

3. OPEN LOOP SIMULATIONS

A set of $(N+3)$ differential equations are obtained by an N-mode approximation from the Lagrange's equations. Therefore, the four-bar mechanism system is governed by a total of $(N+3)$ differential and two algebraic constraint equations. As it is well known solving differential-algebraic equations numerically is a challenging task. For simulations presented here an IMSL subroutine (DASPG) which is based on Petzold–Gear method is used [12]. The number of modes to be taken to guarantee convergence depends on the type of excitations. Since the primary objective of this study is to investigate the feasibility of controlling the vibrations through the input link, a smooth sinusoidal torque input is used to drive the system. In this case only the first mode is dominant. Therefore, a two-mode approximation is considered to be adequate. For comparison purposes, another set of simulations was carried out by assuming that the coupler link behaves as rigid (i.e., neglecting the elastic deformations). The values of the parameters used in the simulations are given in Table 1. The torque input is given by

$$\tau(t) = \begin{cases} \tau_0\sin(2\pi t/T_m) & t \leqslant T_m, \\ 0 & t \geqslant T_m, \end{cases} \tag{17}$$

where τ_0 is the peak torque and T_m is the duration of the torque.

Figures 2–5 compare open-loop responses of rigid and flexible mechanism with a peak torque magnitude of $\tau_0 = 0{\cdot}003$ Nm and $T_m = 1$ s. As mentioned in

TABLE 1
Parameters used in the simulations

Constant	Description	Value
l_1	Length of the ground link	0·4064 m
l_2	Length of the input link	0·0635 m
l_3	Length of the coupler link	0·3048 m
l_4	Length of the output link	0·3048 m
I_c	Moment of inertia of the input link	$2{\cdot}002 \times 10^{-3}$ kgm^2
I_o	Moment of inertia of the output link	$7{\cdot}46 \times 10^{-6}$ kgm^2
ρ	Mass per unit length	0·2237 kg/m
E	Modulus of elasticity	$2{\cdot}06 \times 10^{11}$ Pa
I	Area moment of inertia of the coupler link	$5{\cdot}34 \times 10^{-12}$ m^4
m_2	Mass of the input link	0·0142 kg
m_3	Mass of the coupler link	0·0682 kg
m_4	Mass of the output link	0·0682 kg

section 1, because of the fully coupled nature of the equations, the rigid body co-ordinates (e.g., input and output link angular displacements) are affected by the elastic deformation of the coupler link. However, this effect is negligible and can only be seen in the joint angular velocities (see Figures 4 and 5).

Another set of simulations are carried out with a peak torque magnitude of $\tau_0 = 0{\cdot}01$ Nm and $T_m = 1$ s. The open-loop responses for the flexible and rigid models of the four-bar mechanism are shown in Figures 6 through 9. The effect of flexibility is now more pronounced, since the larger torque causes larger

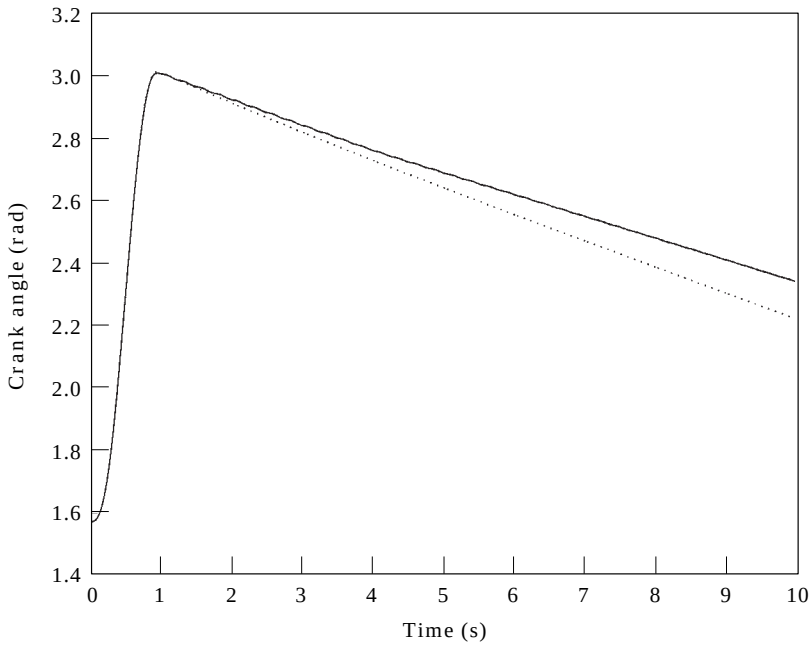

Figure 2. Crank angle open-loop time response, $\tau_0 = 0{\cdot}003$ Nm; —, flexible; ..., rigid.

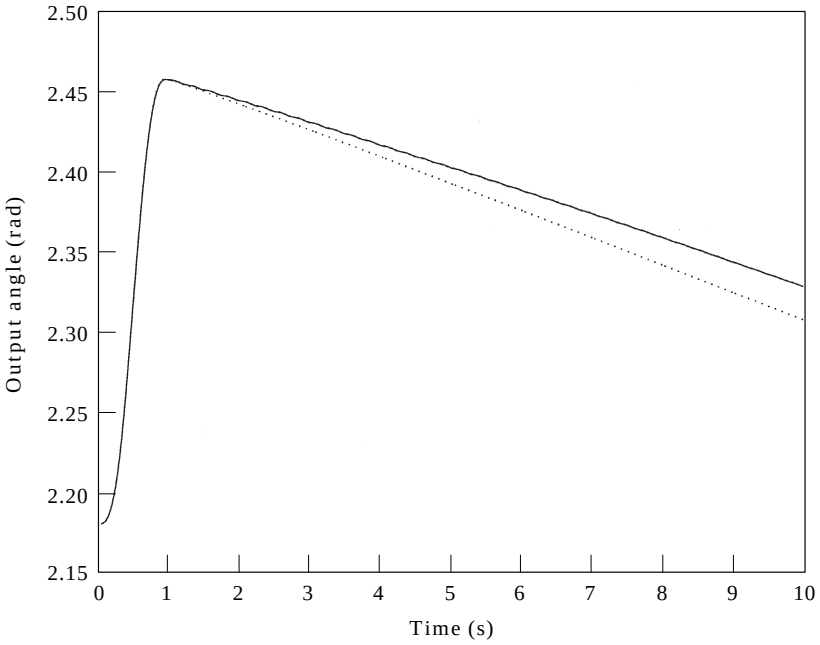

Figure 3. Output angle open-loop time response, $\tau_0 = 0{\cdot}003$ Nm; key as Figure 2.

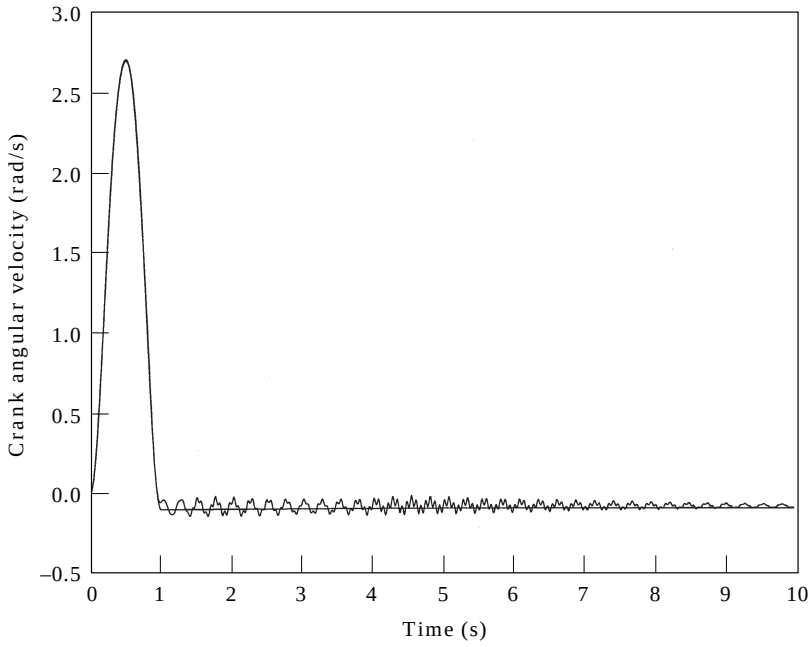

Figure 4. Crank angular velocity open-loop time response, $\tau_0 = 0{\cdot}003$ Nm; key as Figure 2.

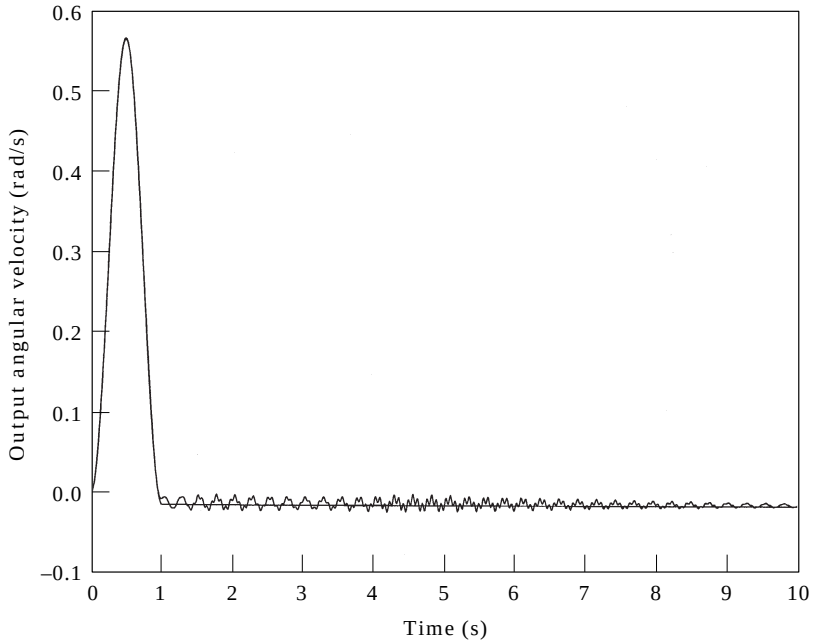

Figure 5. Output angular velocity open-loop time response, $\tau_0 = 0{\cdot}003$ Nm; key as Figure 2.

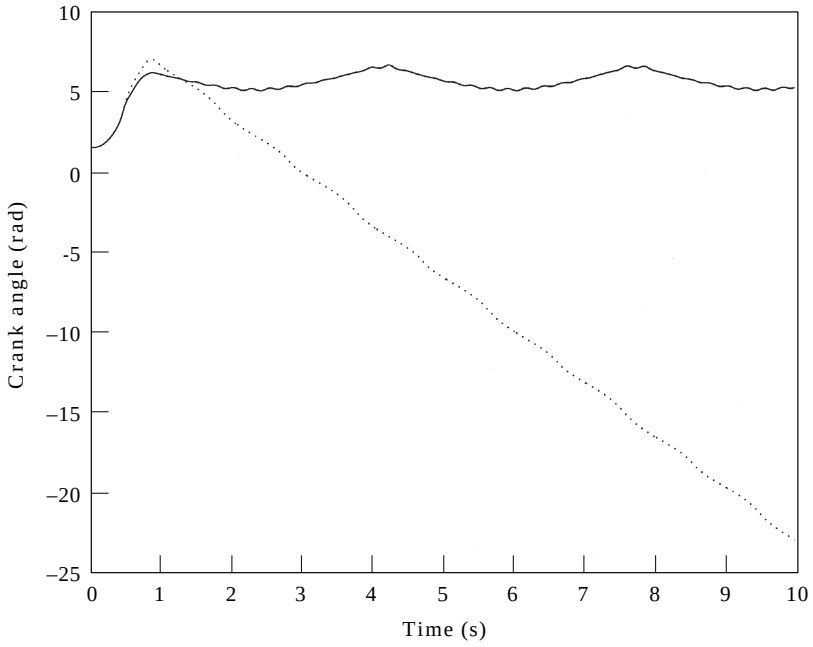

Figure 6. Crank angle open-loop time response, $\tau_0 = 0{\cdot}01$ Nm; key as Figure 2.

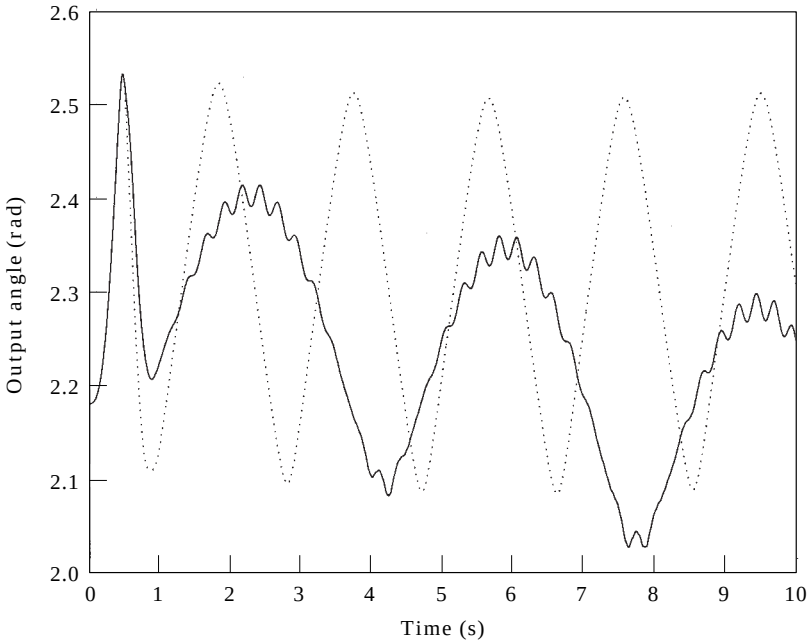

Figure 7. Output angle open-loop time response, $\tau_0 = 0{\cdot}01$ Nm; —, flexible; key as Figure 2.

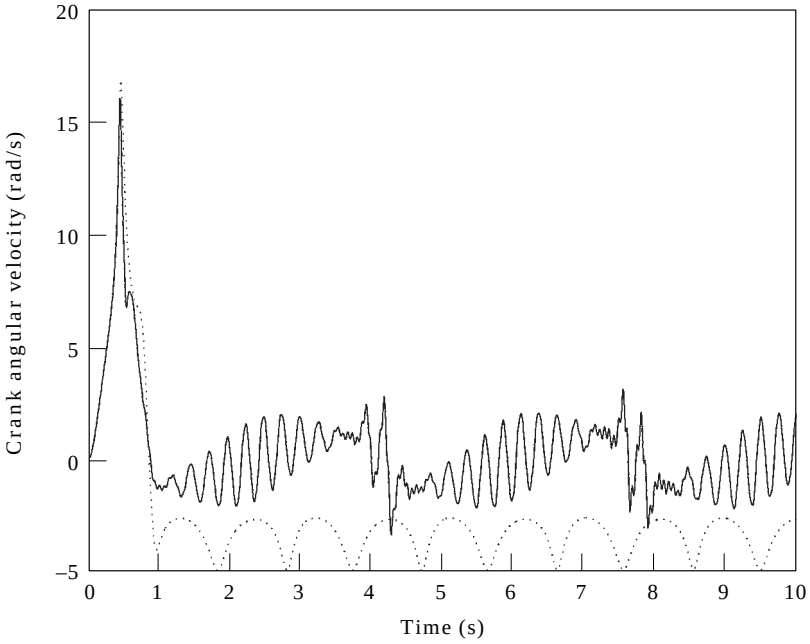

Figure 8. Crank angular velocity open-loop time response, $\tau_0 = 0{\cdot}01$ Nm; key as Figure 2.

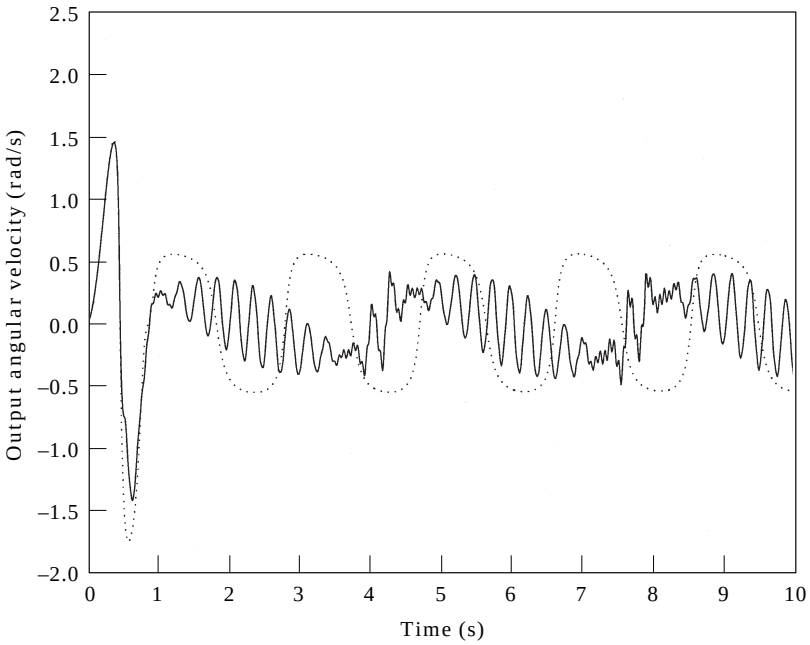

Figure 9. Output angular velocity open-loop time response, $\tau_0 = 0{\cdot}01$ Nm; key as Figure 2.

elastic deformations. The effect of flexibility is significant not only on the joint angular velocities, but also on the joint angles. Clearly, in this case, a rigid model or a flexible model without full coupling will yield gross errors with respect to rigid body motions since the effect of elastic deformation will not be seen in rigid body co-ordinates.

It is apparent from Figures 2 through 9 that the flexibility of the coupler link is felt in the input as well as the output links. This makes it possible to suppress the vibrations of the coupler link through the input torque. However, it is clear that models based on decoupled rigid and flexible motions cannot be used for the proposed type of control.

4. CONTROL DESIGN AND CLOSED LOOP SIMULATIONS

The governing equations are highly non-linear differential equations. Most control designs require a linear unconstrained model. In this case a straightforward linearization is not possible since it may be difficult to find an operating point. However, the equations can be linearized around an open-loop rigid body trajectory. Since the main goal of the controller is to suppress vibrations, a rigid body trajectory can be used as the nominal trajectory and the deviations from this can be assumed small.

For small deviations from the open-loop trajectory, the constraint equations can also be linearized to obtain an expression for the coupler and output angles as a function of the input angle. A set of unconstrained linear system of differential equations describing the mechanism for a small motion range can be

obtained as follows: Let:

$$\theta_2 = \theta_{2e} + \delta\theta_2, \quad \theta_3 = \theta_{3e} + \delta\theta_3, \quad \theta_4 = \theta_{4e} + \delta\theta_4,$$

where θ_{2e}, θ_{3e}, θ_{4e} represent the open-loop trajectory. Using the constraint vector $\mathbf{\Phi}$ given in equation (9), one can obtain the deviations from the open-loop trajectory $\delta\theta_3$ and $\delta\theta_4$ as a function of $\delta\theta_2$ as:

$$\delta\theta_3 = -\frac{l_4 - l_3\cos(\theta_{3e} - \theta_{4e}) + l_1\cos(\theta_{3e}) - l_2\cos(\theta_{2e} - \theta_{3e})}{l_2\sin(\theta_{3e} - \theta_{4e})} - \frac{l_4\sin(\theta_{2e} - \theta_{3e})}{l_2\sin(\theta_{3e} - \theta_{4e})}\delta\theta_2. \tag{18}$$

$$\delta\theta_4 = -\frac{-l_3 + l_1\cos(\theta_{3e}) - l_2\cos(\theta_{2e} + \theta_{3e})}{l_3\sin(\theta_{3e} - \theta 4e)} - \frac{l_4\cos(\theta_{2e} - \theta_{3e}) + l_2\sin(\theta_{2e} - \theta_{3e})}{l_3\sin(\theta_{3e} - \theta_{4e})}\delta\theta_2. \tag{19}$$

Replacing these linearized constraint equations in the linearized equations of motion, the resultant unconstrained equations can be written as follows:

$$\bar{M}\delta\ddot{\eta} + \bar{C}\delta\dot{\eta} + \bar{K}\delta\eta = \delta Q, \tag{20}$$

where $\bar{M}$, $\bar{C}$, and $\bar{K}$ are the associated condensed matrices, and

$$\delta\eta^T = [\delta\theta_2 \quad q_1 \quad q_2 \quad \dots \quad q_n]^T, \tag{21}$$

$$\delta Q^T = [\tau_c \quad 0 \quad \dots \quad 0]^T, \tag{22}$$

where τ_c is the control torque applied to the input link.

In order to investigate whether it is possible to suppress vibrations of the flexible link by a control torque applied to the input link, a simple control strategy is tried. The control torque is given by

$$\tau_c = -K_p\delta\theta_2 - K_d\delta\dot{\theta}_2, \tag{23}$$

where K_p and K_d are the controller gains and $\delta\theta_2$ is given by:

$$\delta\theta_2 = \theta_2(t) - \theta_{2d}(t), \tag{24}$$

where $\theta_{2d}(t)$ is the desired input angle profile which can be taken as the desired open-loop rigid body trajectory. The chosen control scheme employs a motor for actuation, an encoder for the sensor, all placed at the input link joint. This type of control arrangement makes real time implementation easy.

For the first set of simulations, the desired trajectory is assumed to be a constant (regulator type of problem) resulting in a constant set of operation angles (i.e., zero open-loop input torque). The system is disturbed by an initial deflection of the coupler. The control objective is to suppress the vibrations while keeping the mechanism's input, coupler, and output angles unchanged.

The initial controller gains are obtained using the linear model and the pole placement technique (the poles are chosen to be $s = -21 \pm 38{\cdot}5i,\ -7{\cdot}5 \pm 3i$). The gains associated with the chosen poles are found to be: $K_p = 0{\cdot}008$ and $K_d = 0{\cdot}002$; however, these gains are tuned using the nonlinear constrained model as $K_p = 0{\cdot}08$ and $K_d = 0{\cdot}004$.

Figures 10 through 12 show the performance of a PD controller. For these simulations, the system is excited by an initial mid-point deflection of 4 mm. Both open and closed-loop responses are shown. For the open-loop simulations, there is no torque input applied. The initial deflection in the coupler link results in some initial velocities which cause the joint angles to grow. In other words, part of the initial elastic energy is transferred to the rigid body motion. This clearly shows the interaction between the elastic deformations and the rigid body motion. In the closed-loop case, the energy transferred from the elastic deformation to the joint motion is absorbed by the control action. Consequently, the vibrations are suppressed and the rigid body motion is stopped. In short, the controller is able to suppress the vibrations and control the link angular motions. The required control torque is shown in Figure 13.

Next, another set of simulations are performed by requiring the input angle to follow a desired trajectory for a rest to rest maneuver while suppressing the vibrations of the coupler link. The desired trajectory is selected as

$$\theta_{2d}(t) = \begin{cases} \theta_{2e} + t - \sin\left(\frac{2\pi t}{T_m}\right), & t < T_m, \\ \theta_{2e} + T_m, & t > T_m, \end{cases} \tag{25}$$

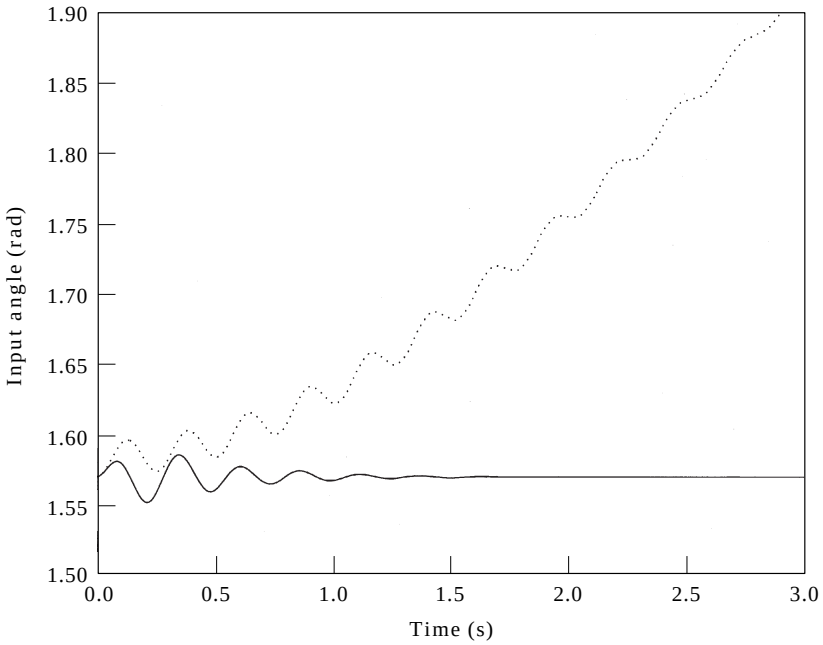

Figure 10. Time response with PD control for the regulator problem, the input angle; θ_2; —, closed-loop; . . . , open-loop.

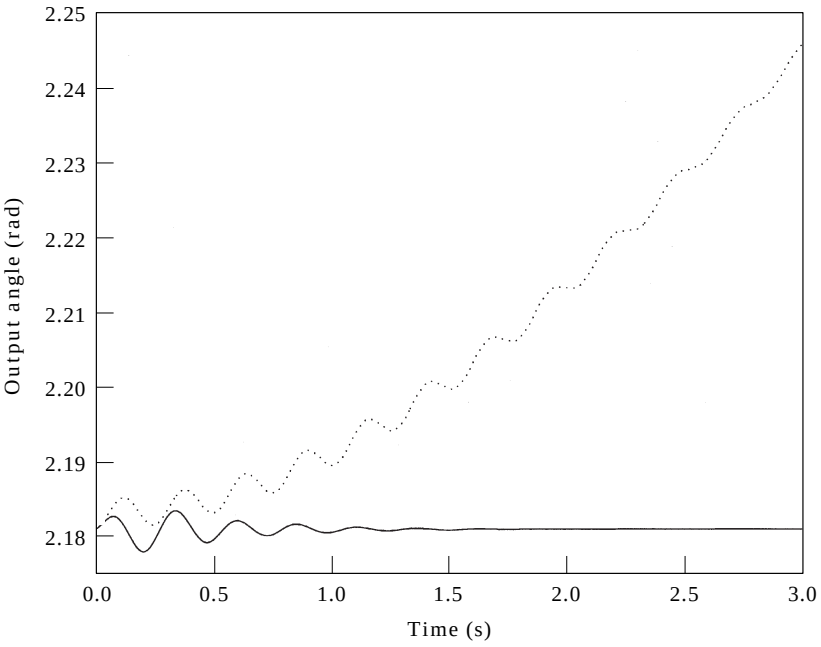

Figure 11. Time response with PD control for the regulator problem, the output angle, θ_4; key as Figure 10.

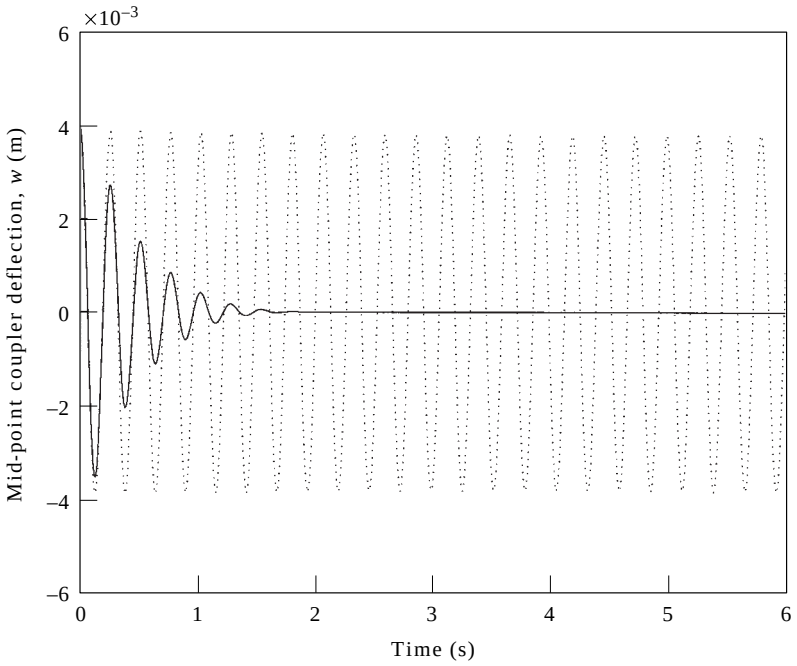

Figure 12. Time response with PD control for the regulator problem, coupler mid-point deflection, w; key as Figure 10.

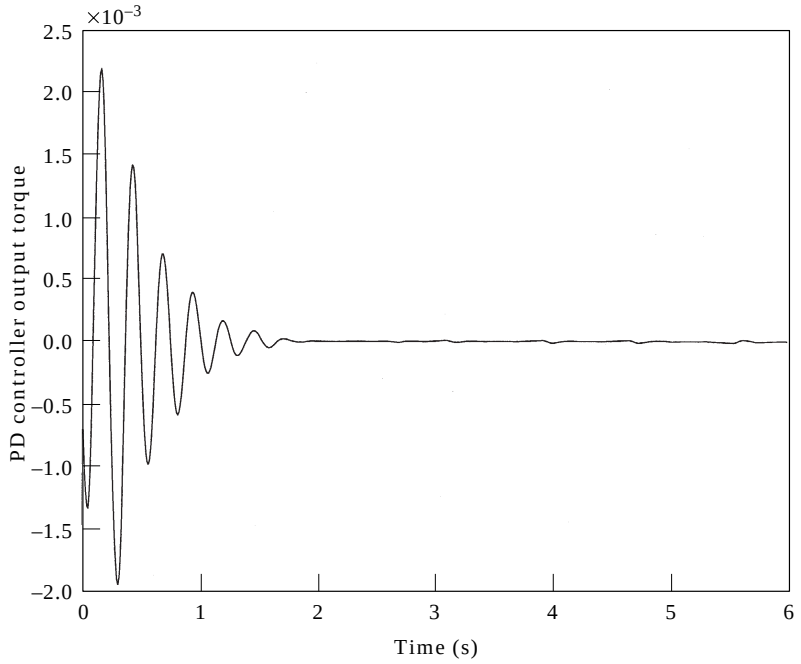

Figure 13. PD controller output torque.

where T_m is the duration of the maneuver. In order to evaluate the performance of the controller, an open-loop input torque profile which would result in a similar input and output angle is used to obtain the open-loop response. Note that no inverse dynamics procedure is used to prescribe the open-loop torque. The purpose here is to investigate the performance of the closed-loop and to provide quantitative comparisons with respect to the required control action. Figures 14–16 show both open and closed-loop responses. The search for the controller gains is done using the linear and non-linear models as in the previous controller design. The PD controller gains are found to be $K_p = 0{\cdot}05$ and $K_d = 1{\cdot}0$. With the designed controller in place, the desired trajectory is followed with very good accuracy. The vibrations are suppressed within 2 s, and the final position is reached without any significant vibration. It is clear that the proposed controller results in a very good closed-loop behavior without requiring excessive control effort as can be seen by comparing open and closed-loop torques (see Figure 17).

Proportional plus derivative (PD) control essentially imitates a passive controller and thus it is unconditionally stable. In fact, it can be thought of as a variable coefficient torsional spring and damper. Since it does not require measurements of the elastic deformations, there is no problem of spillover [13]. However, the performance of a PD controller is limited by the first modal frequency of the elastic link, i.e., it can not be made arbitrarily fast [14]. This is because there is no feedback of elastic deformations, and therefore the closed-loop frequencies related to flexible motion can not be altered. Furthermore, the performance will not be robust for a wide range of input angles because of the

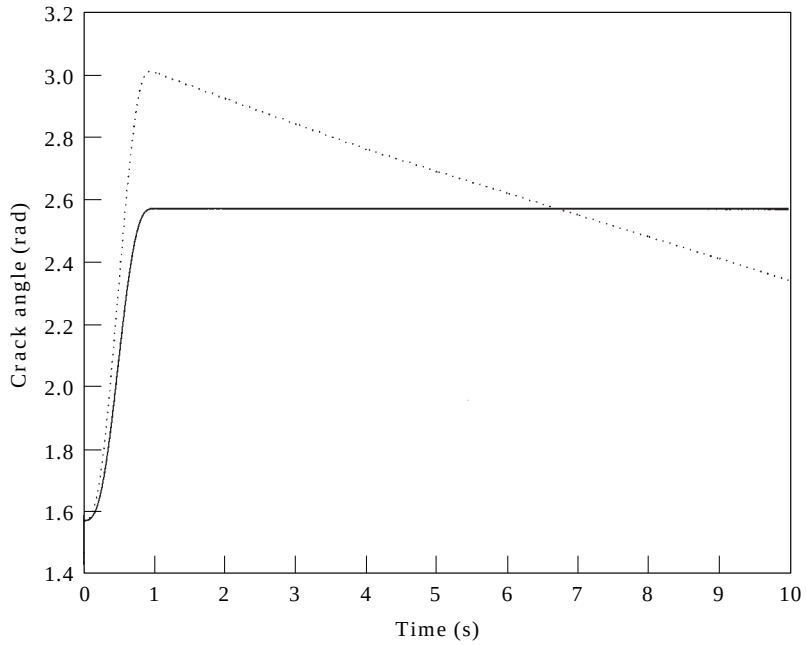

Figure 14. Time response with PD control for start-stop input command, the crank angle, θ_2; key as Figure 10.

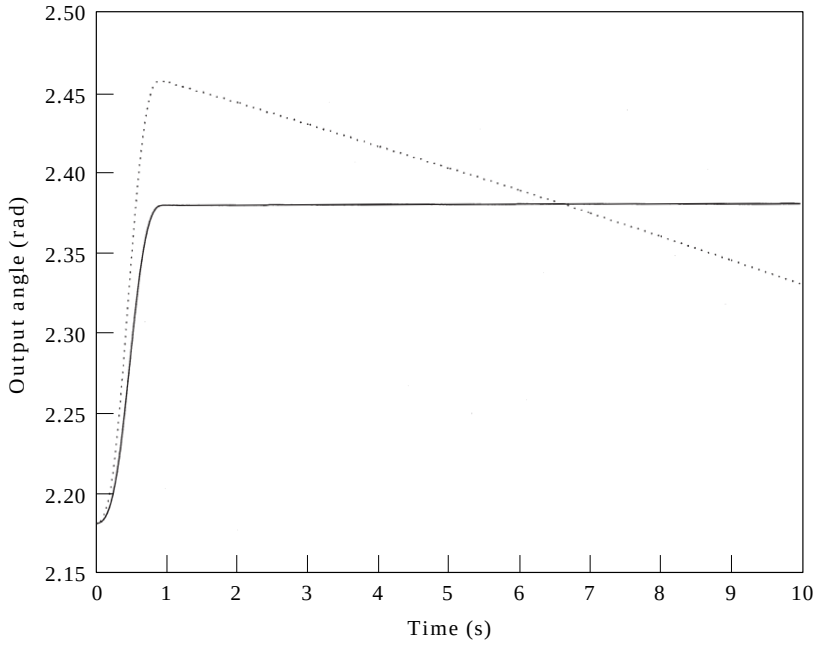

Figure 15. Time response with PD control for start–stop input command, the output angle, θ_4; key as Figure 10.

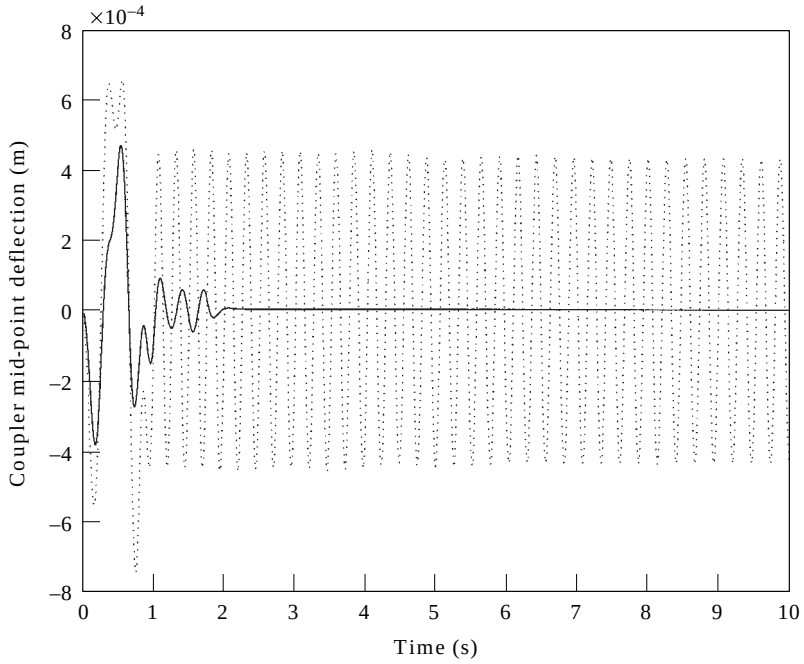

Figure 16. Time response with PD control for start-stop input command, the coupler mid-point deflection, w; key as Figure 10.

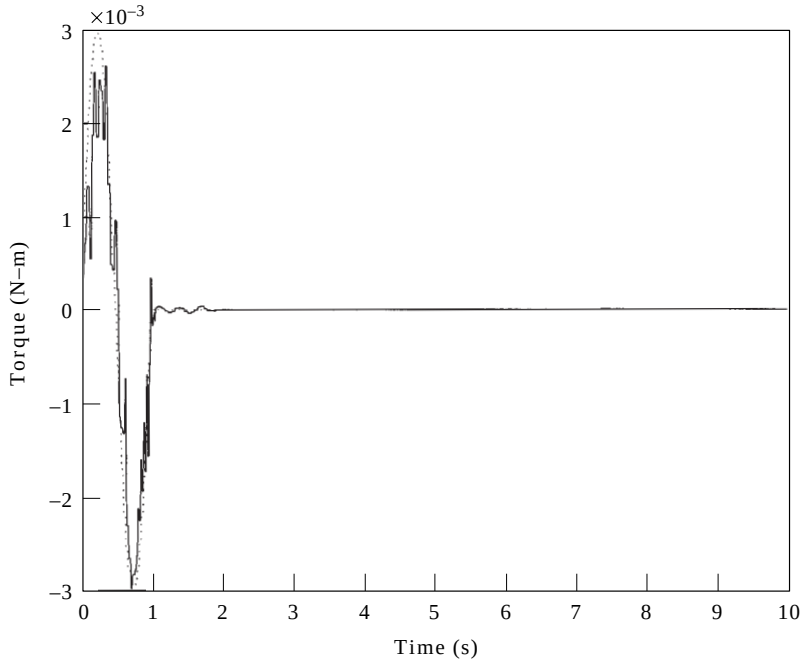

Figure 17. Open-loop and closed-loop torques for start-stop input command; key as Figure 10.

effect of non-linearities and varying coefficients. Despite these limitations, however, the controller can be easily implemented due to its simplicity. The performance can be improved by gain scheduling where several sets of gains are used for a large angle maneuver.

5. CONCLUSIONS

Modelling and control of a flexible four-bar mechanism has been investigated. Governing non-linear equations are obtained through a constrained Lagrangian approach. The equations are fully coupled such that the mutual dependence between rigid body and elastic motions is preserved. Resulting differential-algebraic equations are solved numerically to simulate the system open-loop and closed-loop behavior. A linearized dynamic model is developed which facilitates design of a simple PD controller which does not require measurement of the elastic deformations. The gains obtained are used as initial estimates for controlling the actual mechanism system described by a set of coupled non-linear differential-algebraic equations. The resultant controller has been shown to be efficient in suppressing the vibrations of the flexible link as well as controlling the rigid body motion. The work is ongoing to improve the performance of the proposed controllers by gain scheduling.

REFERENCES

1. G. N. SANDOR and A. G. ERDMAN 1984 *Advanced Mechanism Design: Analysis and Synthesis*. Englewood Cliffs, NJ: Prentice-Hall.
2. A. A. SHABANA 1989 Dynamics of Multibody Systems, New York: Wiley-Interscience.
3. S. NAGARAJAN and D. A. TURIC 1990 *Journal of Dynamic Systems, Measurement and Control* **112**, 203–224. Lagrangian formulation of the equations of motion for elastic mechanisms with mutual dependence between rigid body and elastic motions, part 1: element level equations, part 2: system equations.
4. W. SUNADA and S. DUBOWSKY 1981 *Journal of Mechanical Design* **103**, 643–651. The application of finite element methods to the dynamic analysis of spatial and co-planar linkage systems.
5. A. L. SCHWAB and J. P. MEIJARD 1997 *Proceedings of the* 1997 *ASME Design Engineering Technical Conferences, Sacramento, CA*, 1–7. Small vibrations superimposed on non-linear rigid body motion.
6. A. YIGIT, R. A. SCOTT and A. G. ULSOY 1988 *Journal of Sound and Vibration* **121**, 201–210. Flexural motion of a radially rotating beam attached to a rigid body.
7. H. EL-ABSY and A. A. SHABANA 1996 *Journal of Sound and Vibration* **198**, 617–637. Coupling between rigid body and deformation modes.
8. Y. A. KHULIEF and A. A. SHABANA 1986 *ASME Journal of Mechanisms, Transmissions, and Automation in Design* **108**, 38–45. Dynamic analysis of constrained system of rigid and flexible bodies with intermittent motion.
9. C. K. SUNG and Y. C. CHEN 1991 *ASME Journal of Vibration and Acoustics* **113**, 14–21. Vibration control of the elastodynamic response of high-speed flexible linkage mechanisms.
10. D. G. BEALE and S. W. LEE 1995 *ASME Design Engineering Technical Conferences* **DE-Vol. 84–1**, 203–209. The applicability of fuzzy control for flexible mechanisms.

11. W. H. LIAO, J. H. CHOU and I. R. HORNG 1997 *Smart Materials and Structures* **6**, 457–463. Robust vibration control of flexible linkage mechanisms using piezoelectric films.
12. C. W. Gear and L. R. PETZOLD 1984 *Journal of Numerical Analysis* **21**, 716–728. ODE methods of the solution of differential/algebraic systems.
13. M. J. BALAS 1978 *IEEE Transactions on Automatic Control* **AC-23**, 673–679. Feedback control of flexible systems.
14. A. S. YIGIT 1994 *ASME Journal of Dynamic Systems, Measurement, and Control* **116**, 208–215. On the stability of PD control for a two-link rigid-flexible manipulator.